Structure−Activity Relationships of α-Ketooxazole Inhibitors of Fatty Acid Amide Hydrolase

Christophe Hardouin,[†,‡] Michael J. Kelso,[†,‡] F. Anthony Romero,[†,‡] Thomas J. Rayl,[†,‡] Donmienne Leung,[‡,§] Inkyu Hwang,[†,‡] Benjamin F. Cravatt,[‡,§] and Dale L. Boger*[,†,‡]

Departments of Chemistry and Cell Biology and The Skaggs Institute for Chemical Biology, The Scripps Research Institute, 10550 North Torrey Pines Road, La Jolla, California 92037

Received December 8, 2006

A systematic study of the structure−activity relationships of **2b** (OL-135), a potent inhibitor of fatty acid amide hydrolase (FAAH), is detailed targeting the C2 acyl side chain. A series of aryl replacements or substituents for the terminal phenyl group provided effective inhibitors (e.g., **5c**, aryl = 1-napthyl, K_i = 2.6 nM), with **5hh** (aryl = 3-ClPh, K_i = 900 pM) being 5-fold more potent than **2b**. Conformationally restricted C2 side chains were examined, and many provided exceptionally potent inhibitors, of which **11j** (ethylbiphenyl side chain) was established to be a 750 pM inhibitor. A systematic series of heteroatoms (O, NMe, S), electron-withdrawing groups (SO, SO_2), and amides positioned within and hydroxyl substitutions on the linking side chain were investigated, which typically led to a loss in potency. The most tolerant positions provided effective inhibitors (**12p**, 6-position S, K_i = 3 nM, or **13d**, 2-position OH, K_i = 8 nM) comparable in potency to **2b**. Proteome-wide screening of selected inhibitors from the systematic series of >100 candidates prepared revealed that they are selective for FAAH over all other mammalian serine proteases.

Introduction

The enzyme fatty acid amide hydrolase (FAAH)[a] is the primary catabolic regulator of several bioactive lipid amides in vivo, including anandamide (**1a**) and oleamide (**1b**).[1−4] The central nervous system distribution of FAAH suggests that it degrades neuromodulating fatty acid amides at their sites of action and is intimately involved in their regulation.[5] Fatty acid amide hydrolase is currently the only characterized mammalian enzyme that is in the amidase signature family bearing an unusual catalytic Ser−Ser−Lys triad.[1,4,6−8] Recently, the crystal structure of FAAH cocrystallized with an irreversibly bound arachidonyl fluorophosphonate confirmed its unusual catalytic triad and provided structural details of this enzyme.[1]

Both anandamide (**1a**)[9] and oleamide (**1b**)[10−12] have emerged as prototypical members of the class of bioactive lipid amides[13,14] that serve as chemical messengers (Figure 1). Anandamide, the most recognized member of the endogenous fatty acid ethanolamides,[15] binds and activates both the central type 1 (CB1) and peripheral type 2 (CB2) cannabinoid receptors. Anandamide and members of the cannabinoid family[16] have been implicated in the modulation of nociception,[17−19] feeding,[20,21] emesis, anxiety,[22] cell proliferation,[23,24] inflammation,[25] memory,[26] and neuroprotection after brain injury.[27] Thus, the cannabinoids have clinical relevance for analgesia, anxiety, epilepsy, cachexia, cancer, and Alzheimer's disease as well as other neurodegenerative diseases.[28−30]

Oleamide was found to accumulate in the cerebrospinal fluid of animals under conditions of sleep deprivation and to induce physiological sleep in a dose-dependent manner.[10,12] It modulates serotonergic systems[31−33] and GABAergic transmission,[34,35] decreases body temperature and locomotor activity,[36] and blocks

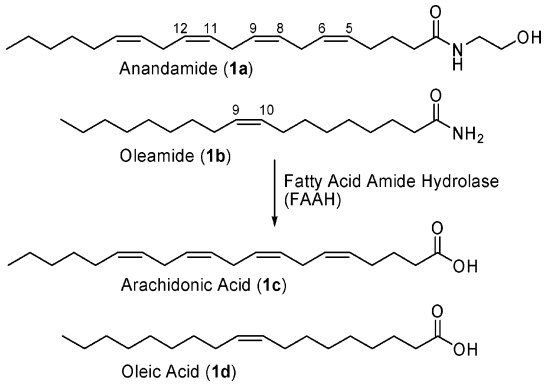

Figure 1. Substrates of FAAH.

glial gap junction cell−cell communication.[37,38] The dual inhibition of presynaptic Na^+ channels and postsynaptic $GABA_A$ receptors suggests that oleamide may possess a mode of action common to drugs that are widely used for the treatment of anxiety, sleep disorders, and epilepsy and that it represents an endogenous ligand for such depressant drug sites in the mammalian brain. Oleamide decreases body temperature and locomotor activity[36] and exhibits the characteristic in vivo analgesic and cannabinoid behavorial effects of anandamide,[31,39] albeit without apparent cannabinoid receptor activation. It has been suggested that the cannabinoid behavorial effects of oleamide may be mediated through an as yet unknown distinct pharmacological target.[34] Because oleamide may play an important role in sleep, it may provide opportunities for the development of sleep aids that induce physiological sleep lacking the side effects of the sedative hypnotics (e.g., the benzodiazepene class), which include rebound insomnia, anterograde amnesia, and suicide abuse potential.

The pharmacological actions of anandamide and oleamide are terminated by FAAH (Figure 1).[1−4] Studies with FAAH knockout mice have shown not only that FAAH is a key regulator of fatty acid amide signaling in vivo, but that the animals exhibit a significantly augmented behavioral response (e.g., increased analgesia, hypomotility, catalepsy) to adminis-

* To whom correspondence should be addressed. Phone: (858) 784-7522. Fax: (858) 784-7550. E-mail: boger@scripps.edu.
† Department of Chemistry.
‡ The Skaggs Institute for Chemical Biology.
§ Department of Cell Biology.

[a] Abbreviations: FAAH, fatty acid amide hydrolase; TGH, triacylglycerol hydrolase.

10.1021/jm061414r CCC: $37.00
Published on Web 06/09/2007

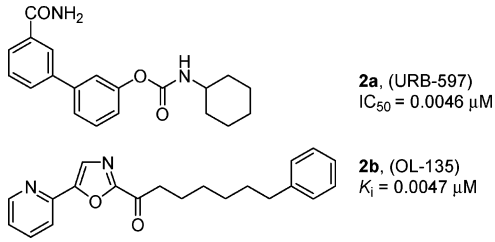

Figure 2. FAAH inhibitors.

tered anandamide and oleamide that correlated with a CB1-dependent analgesic phenotype.[40−43] As such, FAAH has emerged as an interesting new therapeutic target for a range of clinical disorders.[16,44]

Due to the exciting therapeutic potential of inhibiting FAAH, there has been increasing interest in the development of potent inhibitors (Figure 2).[22,45−60] These include the discovery that the endogenous sleep-inducing molecule 2-octyl α-bromoacetoacetate is an effective FAAH inhibitor,[55] a series of reversible inhibitors bearing an electrophilic ketone[46,54,56] (e.g., trifluoromethyl ketone-based) that have not proven selective for FAAH over other mammalian serine hydrolases[61] and a set of irreversible inhibitors[48−50,52,53] (e.g., fluorophosphonates and sulfonyl fluorides). Recently, two classes of inhibitors have been disclosed that provide significant opportunities for the development of an inhibitor with therapeutic potential. One class is the aryl carbamates (e.g., **2a**; Figure 2) that acylate an active site catalytic serine and which were shown to exhibit anxiolytic activity and induce analgesia.[22,57−59,62] However, the selectivity of such aryl carbamate inhibitors is low, and recent studies illustrate that either no or minimal selectivity is achieved (e.g., other targets of **2a** are carboxylesterase 6 and triacylglyceride hydrolase).[63−65] A second class is the α-ketoheterocycle-based inhibitors, some of which are extraordinarily potent (e.g., **2b**; Figure 2).[45,47,51,61,66] These competitive inhibitors bind to FAAH via reversible hemiketal formation with an active site serine, and not only are they potent and extraordinarily selective for FAAH versus other mammalian serine hydrolases,[45,61] but many are efficacious in vivo and promote analgesia.[64,67]

From these latter studies, **2b** has emerged as a lead for further study.[45,51,61,64,66] It has been shown that **2b** is a potent and selective FAAH inhibitor that induces analgesia by raising endogenous anandamide levels,[64] is ≥300-fold selective for FAAH over any other serine hydrolase,[45] lacks significant offsite target activity when surveyed against a panel of receptors and enzymes (Cerep assay profiling), and does not significantly inhibit common P450 metabolism enzymes (3A4, 2C9, 2D6) or the human ether-a-go-go-related gene (hERG). Consequently, we embarked on a more extensive study of the structure−activity relationships (SARs) of **2b**. We recently reported a detailed study targeting the 5-position of the central oxazole of **2b** (e.g., aryl and nonaromatic substituents) and disclosed a series of extraordinarily potent (as low as 400 pM) and selective FAAH inhibitors.[68,69] Herein we report the synthesis and evaluation of a systematic series of α-ketooxazole inhibitors that extensively explores the C2 acyl side chain of **2b** along with results of the proteome-wide selectivity screening of the candidate inhibitors.[70]

Chemistry

The majority of the candidate inhibitors were prepared by one of two methods (Scheme 1). Sonogashira coupling (method A) of **3a**[45] or **3b**[45] with a series of aryl iodides afforded inhibitors **4e**, **4f**, **4pp**, **4qq**, **4o**−**4s**, **4rr**, **4ss**, **4x**−**4cc**, and **4gg**−**4jj**.[71] Hydrogenation of the alkyne provided inhibitors **5e**, **5f**, **5o**−**5s**, **5pp**, **5qq**, **5x**−**5cc**, and **5gg**−**5jj**. Alternatively, direct acid chloride acylation (method B) of a Zn/Cu-metalated 5-(pyridin-2-yl)oxazole[72] (**6**) following the protocol of Anderson et al.[73] yielded inhibitors **5a**−**5d**, **5g**−**5l**, **5t**−**5v**, **5nn**, **5oo**, **11a**−**11j**, **12e**, **12g**, **12i**, **12k**, **12n**, and **12p**.

Scheme 1

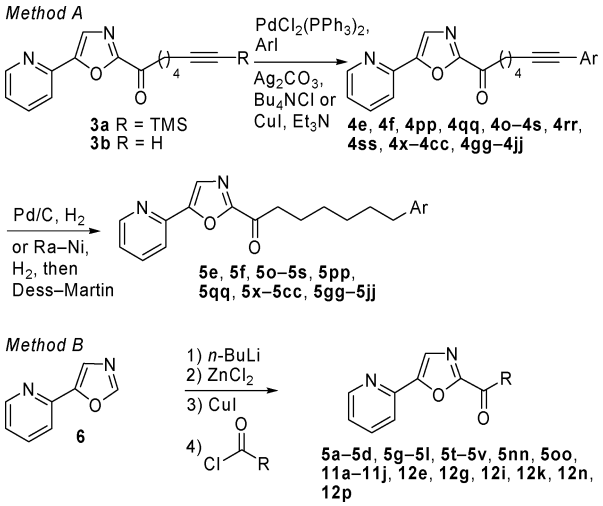

Scheme 2

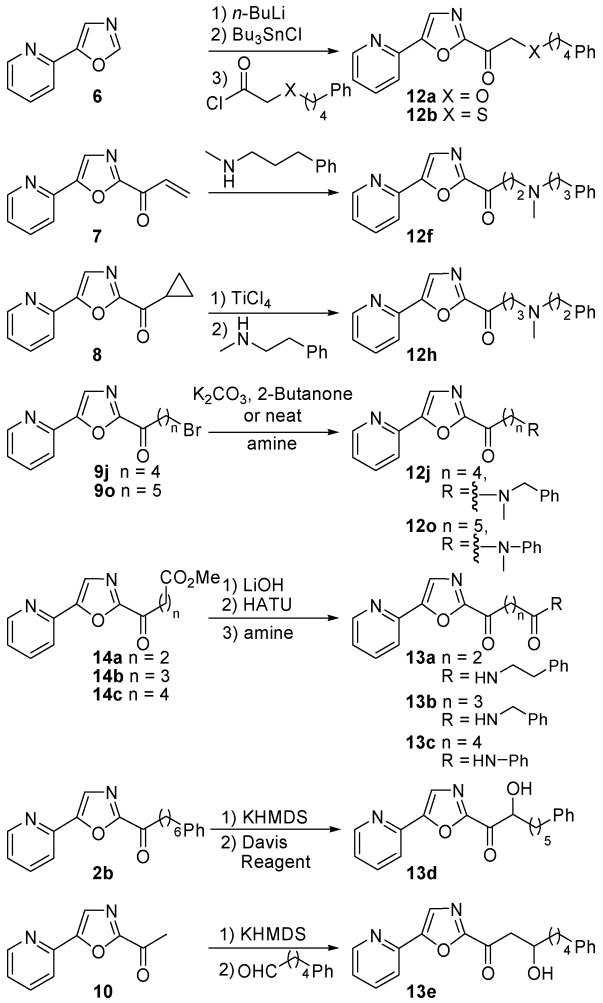

Scheme 2 summarizes the synthesis of the inhibitors that were not prepared by either method A or method B. Oxazole **6** was lithiated at C2, converted to its C2-stannane upon treatment with Bu_3SnCl, and subsequently treated with the corresponding acid

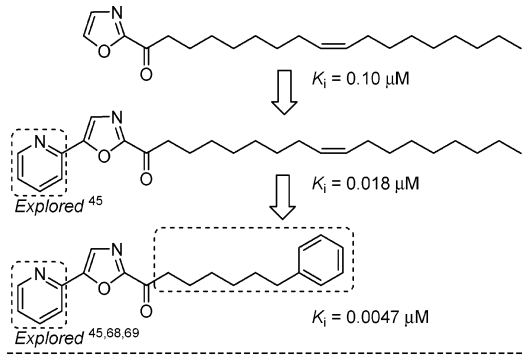

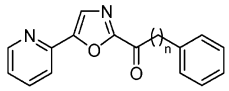

	K_i (μM)	Selectivity (FAAH vs TGH)
n = 3	0.12	N.D.
n = 4	0.033	4
n = 5	0.011	7
n = 6 (**2b**)	0.0047	65 (300)[45]
n = 7	0.0075	125
n = 8	0.008	150
n = 10	0.022	280

•Potency: n = 3 < 4 < 5 < 6 > 7 > 8 > 9 > 10
•Selectivity: n = 10 > 8 > 7 > 6 > 5 > 4

Figure 3. Preceding studies of the C2 side chain.

chloride to afford **12a** and **12b**.[74,75] Compound **12f** was prepared by Michael addition of *N*-methyl-3-phenylpropylamine to enone **7**. Treatment of **8** with $TiCl_4$ followed by *N*-methyl-3-phenylethylamine provided **12h**.[76,77] Compounds **9j** and **9o** were transformed to a series of amino ketones upon treatment with the corresponding amine in the presence of K_2CO_3 in 2-butanone or by treatment with the neat amine. Esters **14a**−**14c** were readily converted to their corresponding amides **13a**−**13c**. α-Hydroxylation of **2b** with the Davis reagent[78] afforded **13d**. Enolization of **10** with KHMDS and subsequent treatment with 5-phenylpentanal yielded **13e**. Inhibitors **5kk**−**5mm**, **12c**, **12d**, **121**, **12m**, **12q**, and **12r** were prepared by oxidation (*m*-CPBA) of the corresponding sulfides **5t**−**v**, **12b**, **12k**, and **12p**.

Enzyme Assay

Enzyme assays were performed at 20−23 °C with purified recombinant rat FAAH expressed in *Escherichia coli*[79] (unless indicated otherwise) or with solubilized COS-7 membrane extracts from cells transiently transfected with human FAAH cDNA[3] (where specifically indicated) in a buffer of 125 mM Tris/1 mM EDTA/0.2% glycerol/0.02% Triton X-100/0.4 mM Hepes, pH 9.0.[55] The initial rates of hydrolysis (≤10−20% reaction) were monitored using enzyme concentrations (typically 1 nM) at least 3 times below the measured K_i by following the breakdown of ^{14}C-oleamide, and K_i values (standard deviations are provided in the Supporting Information tables) were established as described (Dixon plot).[47] Lineweaver−Burk analysis previously established reversible, competitive inhibition for **2b** and related inhibitors.[45]

Results and Discussion

In preceding studies,[45] the length of the linker chain and the incorporation of a terminal phenyl were found to impact and improve inhibitor potency (Figure 3). The linker chain length on compounds related to **2b** exhibited a well-defined parabolic relationship with an optimal length of six carbons terminating in a phenyl group, constituting an overall length of C11

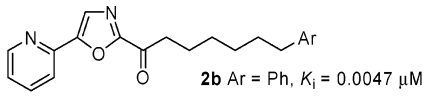

compd	Ar	K_i, μM	compd	Ar	K_i, μM
5a	2-thienyl	0.0043	**5d**	2-naphthyl	0.011
5b	3-thienyl	0.0051	**5e**	2-pyridyl	0.12
5c	1-naphthyl	0.0026	**5f**	3-pyridyl	0.032

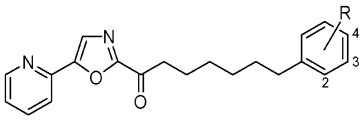

compd	R	K_i, μM	compd	R	K_i, μM
5g	2-CH_3	0.0030	**5x**	2-CF_3	0.004
5h	3-CH_3	0.0033	**5y**	3-CF_3	0.001
5i	4-CH_3	0.0028	**5z**	4-CF_3	0.004
5j	2-OCH_3	0.0058	**5aa**	2-CO_2CH_3	0.001
5k	3-OCH_3	0.0025	**5bb**	3-CO_2CH_3	0.0019
5l	4-OCH_3	0.0062	**5cc**	4-CO_2CH_3	0.0015
5m	3-NH_2	0.030	**5dd**	2-CO_2H	>0.6
5n	4-NH_2	0.0030	**5ee**	3-CO_2H	>0.6
5o	3-NHBOC	0.0024	**5ff**	4-CO_2H	>0.6
5p	4-NHBOC	0.0056	**5gg**	2-Cl	0.0019
5q	2-F	0.0017	**5hh**	3-Cl	0.0009
5r	3-F	0.0022	**5ii**	4-Cl	0.0027
5s	4-F	0.0032	**5jj**	2,3-Cl_2	0.0009
5t	2-SCH_3	0.0033	**5kk**	2-SO_2CH_3	0.037
5u	3-SCH_3	0.0042	**5ll**	3-SO_2CH_3	0.0013
5v	4-SCH_3	0.0025	**5mm**	4-SO_2CH_3	0.019
5w	4-NO_2	0.0065			

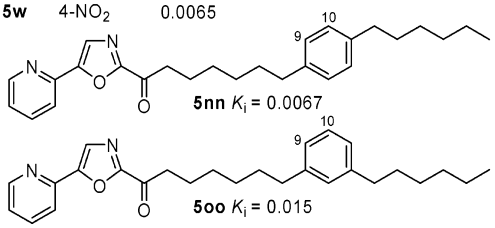

Figure 4. Substitution of the C2 side chain terminal phenyl group.

including the keto group. Slight perturbations on this structure were well tolerated, although shortening the chain length generally led to reduced FAAH selectivity as well as potency, whereas lengthening the connecting chain improved selectivity, but with diminished FAAH potency. The studies herein explore the impact of further altering this C2 acyl side chain of **2b**.

Substitution of the C2 Side Chain Terminal Phenyl Group. A systematic series of aryl replacements and phenyl substitutions for the terminal phenyl group of **2b** were examined (Figure 4). Consistent with expectations based on a modeled FAAH active site analysis surrounding the bound phenyl ring of **2b**,[45] which corresponds to the site of π-interactions with the substrates as well as a bend in their bound conformations ($\Delta^{8,9}$/$\Delta^{11,12}$ double bonds of **1a**, $\Delta^{9,10}$ double bond of **1b**), almost all aryl replacement derivatives (**5a**−**5f**) proved to be effective inhibitors. Both thiophene replacements **5a** and **5b** were indistinguishable from **2b**, the 1-naphthyl substitution **5c** was roughly 2-fold more potent, and the 2-naphthyl derivative **5d** was roughly 2-fold less potent. Incorporation of a more polar pyridine with **5e** and **5f** led to 7−25-fold reductions in K_i, with the 2-pyridyl replacement being the most detrimental to inhibitory potency.

Substitution of the terminal phenyl ring of **2b** was broadly tolerated, and the complete range of *ortho*, *meta*, or *para* substituents that were examined provided effective inhibitors (**5g**−**5oo**, Figure 4). The only exceptions to this generalization were the carboxylic acid derivatives (**5dd**−**ff**) which are deprotonated under the assay conditions (pH 9) and fail to effectively bind in the hydrophobic active site. Typically,

hydrophobic or electron-withdrawing substituents enhanced the binding affinity of the inhibitors more significantly than polar or electron-donating substituents. However, and with a couple of notable exceptions, each substituent enhanced binding affinity indicative of additional favorable binding contacts within the active site. Although this may not be surprising for the hydrophobic substituents (CH_3, CF_3, F, Cl, $SCH_3 \geq OCH_3$, H), it is especially interesting that polar substituents (CO_2CH_3, NO_2, SO_2CH_3, NH_2) can be tolerated in this hydrophobic pocket and that some even enhance inhibitory potency. This appears to be especially true of the *meta* position where even the methyl sulfone **5ll** produced an inhibitor more potent than **2b**, whereas the corresponding *o*- and *p*-methyl sulfone derivatives (**5kk** and **5mm**, respectively) were ≥10-fold less effective. The potency of such derivatives typically ranged from 5 to 0.9 nM (K_i) and displayed a variable and weak preference for the site of attachment, and the most potent members typically were the *meta*-substituted derivatives. Significantly, **5hh** (R = Cl) broke the nanomolar potency barrier, providing a K_i of 900 pM and exceeding the activity of **2b** by 5-fold. Accordingly, this region provides a rich area where substituents or modifications can be introduced to enhance inhibitor potency, impact features contributing to or improving in vivo properties, and substantially enhance selectivity.

Extending an alkyl *meta* or *para* substituent such that the chain mimics the length of oleamide and the aryl ring placement mimics the position, conformation, and π-characteristics of the *cis* $\Delta^{9,10}$ double bond revealed that **5nn** (*para* substituent) matched the potency of **2b** (but did not improve it), whereas **5oo** (*meta* substituent) was less effective. These observations are analogous to the results of previous studies which additionally revealed a significant decrease in activity with an extended alkyl *ortho* substituent.[46]

C2 Side Chain Conformational Constraints. It is clear from an FAAH active site analysis and the inspection of the X-ray structure[1] of a covalently bound arachidonyl fluorophosphonate, the lipid side chain can adopt a C4−C7 *gauche* versus extended conformation accommodating the $\Delta^{5,6}$ double bond of **1a** and possesses sufficient active site space to accommodate bridges linking the C4/C7 *gauche* (*cis*) sites. In an effort to remove the rotatable side chain bonds in **2b**, potentially improving in vivo absorption characteristics, a series of diaryl-containing side chains were examined which constrain the inhibitors in this *gauche* (*cis*) conformation, mimicking the conformation and π-characteristics of the arachidonyl $\Delta^{5,6}$ double bond (Figure 5). A second terminal aryl group was incorporated to overlay with the arachidonyl $\Delta^{11,12}$ double bond and mimic the terminal phenyl group of **2b**. Consistent with this analysis, **11a** proved to be among one of the most potent FAAH inhibitors disclosed herein, surpassing the activity of **2b**. The isomer **11c** was nearly 10-fold less potent, and incorporation of a heteroatom (O) into the side chain β to the carbonyl (**11b** and **11d**) led to dramatic losses in potency despite its inductive electron-withdrawing character that might be expected to enhance the electrophilic character of the carbonyl. A survey of related compounds (**11e**−**11i**, K_i = 1−3 nM) revealed a wide tolerance for the functionality linking the two aryl rings and that its removal with ethylbiaryl **11j** provided an exceptionally potent FAAH inhibitor (K_i = 750 pM).

In a previous study, the α-keto-5-(2-pyridyl)oxazol-2-yls were found to be roughly 5−25-fold less potent than their corresponding oxazolopyridines.[47] Accordingly, **11k** (K_i = 380 pM) was also prepared and found to be roughly 5-fold more potent than **11a**.

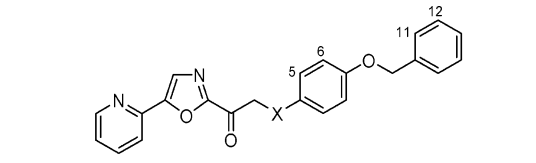

compd	X	K_i, μM	compd	X	K_i, μM
11a	CH_2	0.0013	**11b**	O	5.3

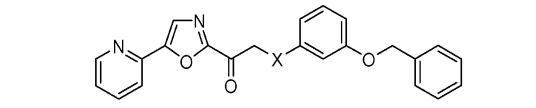

compd	X	K_i, μM	compd	X	K_i, μM
11c	CH_2	0.025	**11d**	O	2.1

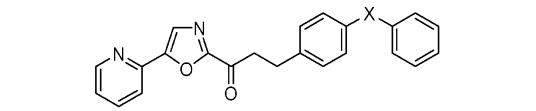

compd	X	K_i, μM	compd	X	K_i, μM
11e	CH_2O	0.001	**11h**	CH_2	0.0032
11f	O	0.0034	**11i**	S	0.0022
11g	NH	0.002	**11j**	–	0.00075

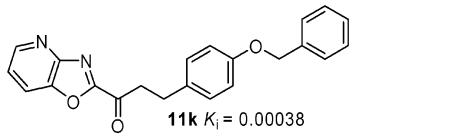

11k K_i = 0.00038

Figure 5. Conformationally restricted C2 side chain inhibitors.

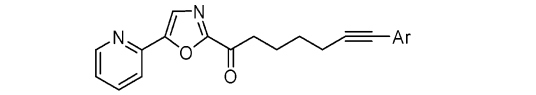

compd	Ar	K_i, μM	compd	Ar	K_i, μM
4e	2-pyridyl	0.28	**4pp**	4-pyridyl	0.15
4f	3-pyridyl	0.3			

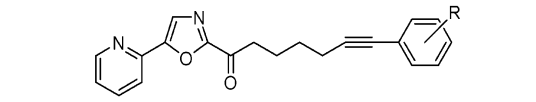

compd	R	K_i, μM	compd	R	K_i, μM
4qq	H	0.025	**4y**	3-CF_3	0.01
4o	3-NHBOC	0.012	**4z**	4-CF_3	0.075
4p	4-NHBOC	0.023	**4aa**	2-CO_2CH_3	0.034
4q	2-F	0.008	**4bb**	3-CO_2CH_3	0.030
4r	3-F	0.0032	**4cc**	4-CO_2CH_3	0.025
4s	4-F	0.036	**4gg**	2-Cl	0.013
4rr	2-NO_2	0.017	**4hh**	3-Cl	0.007
4ss	3-NO_2	0.0048	**4ii**	4-Cl	0.020
4w	4-NO_2	0.031	**4jj**	2,3-Cl_2	0.005
4x	2-CF_3	0.016			

Figure 6. Linker alkynes.

Finally, the alkyne precursors **4** to the series **5** inhibitors prepared by the Shonogashira coupling (method A) were also examined for FAAH inhibition, and the results are summarized in Figure 6. It was observed that there was a 2−20-fold loss in activity with the alkynes compared to their corresponding alkane derivatives (Figure 4), suggesting that this restriction places the terminal aryl ring in a less favorable area in the FAAH active site.

Substitution along the Side Chain. A systematic series of heteroatoms and electron-withdrawing substituents positioned within the linking side chain of **2b** were also investigated (Figure 7). Surprisingly, but consistent with observations made with **11b** and **11d** (Figure 5), placing a heteroatom or electron-withdrawing substituent at the 2-position of the side chain (**12a**−**12d**) β to the electrophilic carbonyl resulted in a dramatic loss in

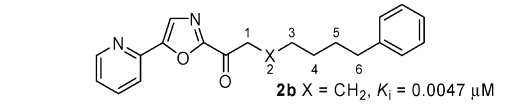

2b X = CH_2, K_i = 0.0047 μM

compd	X	K_i, μM	compd	X	K_i, μM
12a	O	0.06	**12c**	SO	1
12b	S	0.004	**12d**	SO_2	20

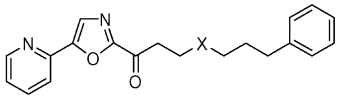

compd	X	K_i, μM	compd	X	K_i, μM
12e	O	0.09	**12f**	NCH_3	0.2

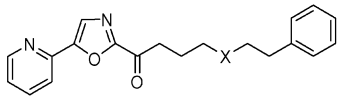

compd	X	K_i, μM	compd	X	K_i, μM
12g	O	0.063	**12h**	NCH_3	3.5

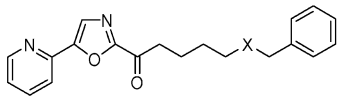

compd	X	K_i, μM	compd	X	K_i, μM
12i	O	0.055	**12l**	SO	2.5
12j	NCH_3	0.20	**12m**	SO_2	>10
12k	S	0.025			

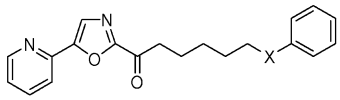

compd	X	K_i, μM	compd	X	K_i, μM
12n	O	0.014	**12q**	SO	1
12o	NCH_3	0.04	**12r**	SO_2	6
12p	S	0.003			

Figure 7. Incorporation of heteroatoms within the side chain.

potency compared to that of **2b** despite its inductive electron-withdrawing character that would be expected to enhance the electrophilic character of the carbonyl. Only the least electronegative atom of the series (X = S, **12b**) matched the potency of **2b**, and the most electronegative functionality (X = SO_2, **12d**) resulted in a 4000-fold loss in potency. A rough trend in K_i is observed as heteroatoms move along the chain where heteroatoms at each end of the chain (2- and 6-positions) are better tolerated than in the middle (3−5-positions). At each location, the substitutions exhibited a well-defined trend of $CH_2 \geq S > O > NMe > SO > SO_2$, albeit in a series that is not complete at each position, clearly reflecting the hydrophobic character of this region of the FAAH active site. Thus, introduction of a sulfur atom provided inhibitors that were comparable in potency to (**12b**, 2-position; **12p**, 6-position) or only slightly less potent than (**12k**, 5-position) **2b**, whereas introduction of an oxygen (>10-fold), NMe (50−100-fold), SO (200−500-fold), and SO_2 (400−1000-fold) led to progressive and substantial losses in binding affinity. At the most tolerant position (position 6), the magnitudes of these effects for sulfur, oxygen, and NMe are dampened, with each providing effective inhibitors.

A series of amides within the linking chain and hydroxyl substitutions on the chain were also explored (Figure 8). Amide placement in the side chain led to a dramatic loss in inhibitory potency (≥1000-fold). Consistent with expectations, **13a**, but not **13b** or **13c**, exists as the stable *N*-acyl hemiaminal, and this is reflected in its inability to inhibit FAAH. Consistent with the previous series of inhibitors (Figure 7), a well-defined trend in K_i is observed as the hydroxyl substitution moves along the side chain where the hydroxyl group at each end of the side chain was better tolerated than those in the middle of the side chain. Within this series, only **13f** (50%, $CDCl_3$) and **13g** (50%, $CDCl_3$) exist in equilibrium with their internal hemiketal. Thus,

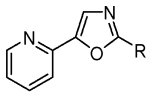

2b R = $(CH_2)_6Ph$, K_i = 0.0047 μM

compd	R	K_i, μM
13a	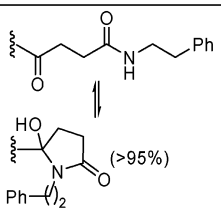	>100
13b	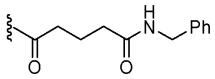	20
13c	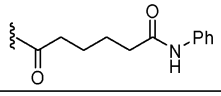	3.1
13d	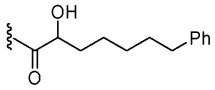	0.008
13e	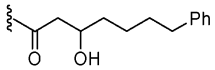	0.035
13f	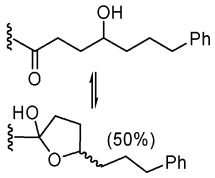	0.5
13g	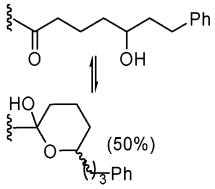	1.5
13h	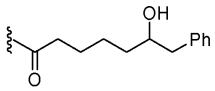	0.2
13i	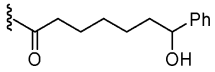	0.035

Figure 8. Hydroxyl and amide substitution.

even though **13f** is 100-fold less potent than **2b**, it may prove useful to examine in vivo where the electrophilic carbonyl would potentially be less prone to metabolic reduction due to the reversible hemiketal formation.

Several additional side chain modifications were examined and represent intermediates or byproducts derived from the synthesis of the preceding candidate inhibitors. The results of their examination are summarized in Figure 9 and highlight several features. Shortening of the side chain and removal of the phenyl group of **2b** with a small series of methyl esters (**14a**−**14c**) led to a significant progressive decrease in potency. The cyclopropyl and cyclopentyl derivatives **14d** and **14e** lacking the extended chain and phenyl group similarly resulted in a loss of activity. Interestingly, and in contrast, the simple α-chloro ketone **14f** was still a submicromolar inhibitor of FAAH although it lacked nearly all of the C2 side chain. Presumably this reflects the inhibitor's increased electrophilic carbonyl reactivity increasing its potency ≥100-fold over that of the inactive methyl ketone[45] (K_i = >100 μM). Placement of a ketone β to the electrophilic carbonyl (**14g**) led to a complete

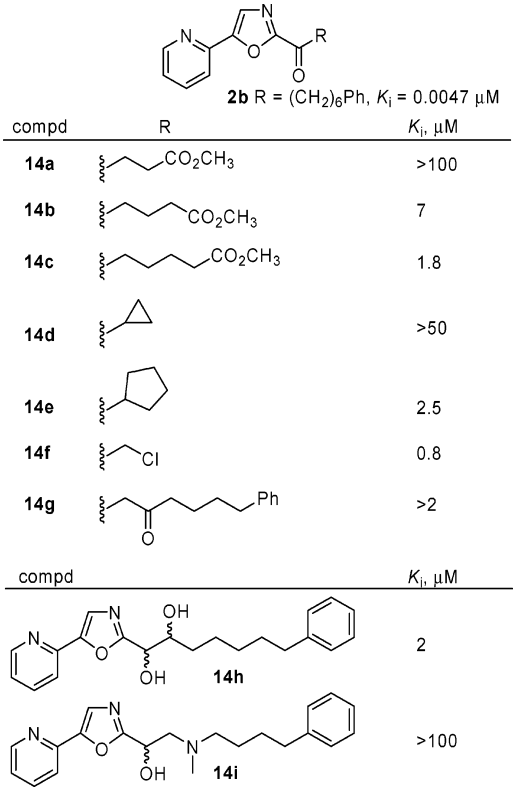

Figure 9. Effect of additional side chain modifications.

compd	K_i, μM (human)	K_i, μM (rat)
5jj	0.0012	0.0009
11a	0.00045	0.0013
11e	0.005	0.001
11j	0.0029	0.00075
11k	0.0006	0.00038

Figure 10. Inhibition of recombinant human fatty acid amide hydrolase.

loss of inhibitory potency compared to **2b**. In this instance, the electrophilic C2 carbonyl of **14g** is enolized (>95%, $CDCl_3$) and unreactive toward nucleophilic attack.

Finally two alcohol derivatives were examined, and consistent with previous observations,[45] **14h** and **14i** both resulted in a substantial loss in inhibitory potency, with **14h** exhibiting a 250-fold loss in activity relative to its corresponding ketone **13d**.

Inhibition of Recombinant Human FAAH. Rat and human FAAHs are very homologous (84% sequence identity), exhibit near identical substrate selectivities and inhibitor sensitivities in studies disclosed to date,[47] and embody an identical amidase signature sequence, suggesting the observations made with rat FAAH would be analogous to those made with the human enzyme. Consequently, key inhibitors in the series were examined against the human enzyme and consistent with previous observations[45,69] were found to exhibit the same relative and absolute potencies (Figure 10).

Selectivity Screening. Early assessments of α-ketoheterocycle inhibitors of FAAH against possible competitive enzymes (e.g., phospholipase A2, ceramidase) revealed no inhibition. Consequently, a method for proteome-wide screening capable of globally profiling all mammalian serine hydrolases was developed,[70] and studies have shown that the α-ketoheterocycle class of inhibitors generally are exquisitely selective for FAAH.[45,61,64] However, two enzymes did emerge as potential competitive targets: triacylglycerol hydrolase (TGH) and an uncharacterized membrane-associated hydrolase that lacks known substrates or function (KIAA1363). In this screen, IC_{50} values are typically higher than the measured K_i values, but the relative potency, the magnitude of binding affinity differences, and the rank order binding determined in the assay parallel those established by standard substrate assays.

compd	K_i, μM	FAAH	KIAA1363	TGH
2b	0.0047	0.002	>100 (>50000)	0.6 (300)
5e	0.12	0.03	>100 (>3300)	1 (33)
5f	0.032	0.02	>100 (>5000)	1(50)
5j	0.0058	0.01	>100 (>10000)	5 (500)
5k	0.0025	0.02	>100 (>5000)	1 (50)
5l	0.0062	0.02	>100 (>5000)	5 (250)
5gg	0.0019	0.02	>100 (>5000)	0.6 (30)
5hh	0.0009	0.002	>100 (>50000)	0.5 (250)
5ii	0.0027	0.03	>100 (>3300)	2 (67)
11a	0.0013	0.001	>100 (>100000)	8 (8000)
11e	0.001	0.002	>100 (>50000)	2 (1000)
11f	0.0034	0.002	>100 (>50000)	0.2 (100)
11g	0.002	0.005	>100 (>20000)	0.6 (120)
11h	0.0032	0.003	>100 (>33000)	0.9 (300)
11i	0.0022	0.002	>100 (>50000)	0.09 (30)
11j	0.0015	0.0007	>100 (>140000)	1.2 (1700)

Figure 11. Selectivity screening, IC_{50}. A full table of results is reported in the Supporting Information.

Summarized in Figure 11 are the results of the selectivity screening of selected candidate inhibitors. In general, the inhibitors, such as **2b**, were very selective for FAAH over TGH and KIAA1361. The pyridyl replacements (**5e**, **5f**) of the terminal phenyl group of **2b** proved very selective for FAAH over KIAA1363, but only moderately selective for FAAH over TGH. Substitution on the terminal phenyl ring of **2b** also provided selective inhibitors, and this was relatively independent of the substitution position (*ortho*, *meta*, or *para*) and whether it was electron-donating or electron-withdrawing (**5j**−**5l** vs **5gg**−**5ii**). Inhibitors that possess the side chain conformational constraints (**11a**, **11e**−**11j**) generally were very selective for FAAH over KIAA1363 and typically 100−1000-fold selective for FAAH over TGH. Most notably, **11a**, **11e**, and **11j** are the most selective inhibitors of the series, surpassing **2b** in both their FAAH potency and selectivity.

Conclusion

In previous studies,[45] the length of the C2 acyl side chain and the incorporation of a terminal phenyl group were found to impact and improve FAAH inhibitor potency, leading to the discovery of **2b**. To more thoroughly explore the C2 side chain of **2b**, an extensive series of more than 100 derivatives were prepared and evaluated for FAAH inhibitory potency as well as FAAH selectivity versus competitive serine proteases (e.g., TGH, KIAA1363). Aryl replacements of the terminal phenyl group of **2b** resulted in effective inhibitors, many of which are indistinguishable from **2b** and notably with **5c** (aryl = 1-napthyl, K_i = 2.6 nM) being ca. 2-fold more potent than **2b**. A large series of phenyl substituents also proved to be effective inhibitors, with hydrophobic or electron-withdrawing *meta* substituents generally enhancing binding affinity to the greatest extent, with **5hh** (aryl = 3-ClPh, K_i = 900 pM) being 5-fold more potent than **2b**. Conformationally restricted C2 side chains of **2b** were examined, and many of these were found to be exceptionally potent, of which **11j** (ethylbiphenyl side chain) is a 750 pM inhibitor of FAAH. A systematic series of heteroatoms (O, NMe, S) and electron-withdrawing groups (SO, SO_2) positioned within the linking side chain of **2b** were investigated, and surprisingly, substitution β to the electrophilic carbonyl led to a dramatic loss in potency. The most tolerant position (position 6) provided effective inhibitors (**12p**, X = S, K_i = 3 nM) comparable to **2b**. A series of amides within the linking chain and hydroxyl substitutions on the chain were also

explored. Amide placement in the side chain led to a dramatic loss in inhibitory potency, whereas hydroxyl substitution at positions 2 and 6 provided effective inhibitors (**13a**, 2-position OH, $K_i = 8$ nM). Just as importantly, proteome-wide selectivity screening of the candidate inhibitors showed extraordinary selectivity for FAAH over all other serine hydrolases and proteases. Most notably, inhibitors that possess the side chain conformational constraints (**11a**, **11e**−**11j**) generally were very selective for FAAH over KIAA1363 and typically 100−1000-fold selective for FAAH over TGH. Finally and despite the lipophilic and non-drug-like nature of the FAAH substrates, the lead structure **2b** and the potent inhibitors disclosed herein including **5hh** and **11j** possess much more favorable drug-like characteristics.[80]

Experimental Section

1-Oxo-1-[5-(2-pyridyl)oxazol-2-yl]-7-(3-chlorophenyl)heptane (5hh). A solution of hept-6-ynoic acid (1.90 g, 14.8 mmol) in anhydrous THF (90 mL) at −78 °C was treated with *n*-BuLi (2.3 M in hexanes, 14.5 mL, 33.3 mmol). After the resulting solution was stirred for 2 min, TMSCl (5.8 mL, 46.0 mmol) was added. The reaction mixture was allowed to warm slowly to 25 °C and was stirred for 1 h. The reaction was quenched with the addition of aqueous 2 N HCl and extracted with CH_2Cl_2. The organic layer was dried over Na_2SO_4, filtered, and concentrated. Column chromatography (SiO_2, 4 × 6 cm, 20% EtOAc−hexanes) afforded 7-(trimethylsilyl)hept-6-ynoic acid (2.7 g, 13.6 mmol, 92%) as a white solid: ^{1}H NMR ($CDCl_3$, 500 MHz) δ 2.40 (t, 2H, $J = 7.4$ Hz), 2.24 (t, 2H, $J = 7.3$ Hz), 1.78−1.72 (m, 2H), 1.62−1.56 (m, 2H), 0.15 (s, 9H).

A solution of 5-(2-pyridyl)oxazole[72] (600 mg, 4.11 mmol) in anhydrous THF (15 mL) at −78 °C was treated dropwise with a solution of *n*-BuLi (2.2 M in hexanes, 2.4 mL, 4.52 mmol) under N_2, and the resulting solution was stirred at −78 °C for 20 min. A solution of $ZnCl_2$ (0.5 M in THF, 18 mL, 8.22 mmol) was added, and the mixture was warmed to 0 °C. After the mixture was stirred at 0 °C for 45 min, CuI (850 mg, 4.46 mmol) was added. After the mixture was stirred at 0 °C for 10 min, a solution of 7-(trimethylsilyl)hept-6-ynoyl chloride (1.2 equiv, prepared from 7-(trimethylsilyl)hept-6-ynoic acid and oxalyl chloride) in anhydrous THF (9 mL) was added dropwise, and the mixture was stirred at 0 °C for an additional 1 h. The reaction mixture was diluted with a 1:1 mixture of hexanes and EtOAc (60 mL) and washed with 15% aqueous NH_4OH (2 × 30 mL), water (30 mL), and saturated aqueous NaCl (30 mL). The organic layer was dried over anhydrous Na_2SO_4, filtered, and evaporated. Column chromatography (SiO_2, 4 × 6 cm, 30% EtOAc−hexanes) afforded 1-oxo-1-[5-(2-pyridyl)-oxazol-2-yl]-7-(trimethylsilyl)hept-6-yne (**3a**; 875 mg, 2.68 mmol, 74%) as a tan oil: ^{1}H NMR ($CDCl_3$, 400 MHz) δ 8.68 (m, 1H), 7.89−7.86 (m, 2H), 7.82 (td, 1H, $J = 7.6$, 1.8 Hz), 7.34−7.31 (m, 1H), 3.15 (t, 2H, $J = 7.3$ Hz), 2.30 (t, 2H, $J = 7.2$ Hz), 1.94−1.86 (m, 2H), 1.68−1.60 (m, 2H), 0.14 (s, 3H); ^{13}C NMR ($CDCl_3$, 100 MHz) δ 187.9, 157.2, 153.2, 150.0, 146.1, 137.0, 126.8, 124.1, 120.3, 106.6, 84.8, 38.4, 27.9, 22.9, 19.6, 0.0; IR (film) ν_{max} 2955, 2867, 2173, 1699, 1603, 1576, 1504, 1469, 1426, 1383, 1249, 1152, 1118, 1083, 1024, 929, 842, 784, 760 cm^{-1}; ESI-TOF-MS *m*/*z* 327.1530 ($C_{18}H_{22}N_2O_2Si + H^+$ requires 327.1523).

A solution of **3a** (570 mg, 1.75 mmol, 1 equiv) in anhydrous THF (6 mL) at 0 °C was treated with a solution of Bu_4NF in THF (1 M, 2.1 mL, 2.1 mmol). After being stirred for 35 min at 0 °C, the reaction mixture was quenched with H_2O and extracted with EtOAc. The organic layer was dried over anhydrous Na_2SO_4, filtered, and evaporated. Column chromatography (SiO_2, 2.5 × 3 cm, 30% EtOAc−hexanes) afforded 1-oxo-1-[5-(2-pyridyl)oxazol-2-yl]-hept-6-yne (**3b**; 340 mg, 1.36 mmol, 77%) as a tan solid: ^{1}H NMR ($CDCl_3$, 500 MHz) δ 8.68−8.66 (m, 1H), 7.89−7.86 (m, 2H), 7.82 (td, 1H, $J = 7.6$, 1.8 Hz), 7.34−7.31 (m, 1H), 3.15 (t, 2H, $J = 7.3$ Hz), 2.27 (td, 2H, $J = 7.2$, 2.7 Hz), 1.96 (t, 2H, $J = 2.7$ Hz), 1.94−1.88 (m, 2H), 1.68−1.62 (m, 2H); ^{13}C NMR ($CDCl_3$, 125 MHz) δ 187.9, 157.2, 153.2, 150.1, 146.2, 137.1, 126.8, 124.1, 120.3, 83.8, 68.7, 38.4, 27.7, 22.9, 18.2; IR (film) ν_{max} 2938, 2867, 2115, 1698, 1603, 1575, 1505, 1470, 1426, 1385, 1283, 1245, 1127, 1086, 1024, 991, 962, 853, 785, 743 cm^{-1}; ESI-TOF-MS *m*/*z* 255.1135 ($C_{15}H_{14}N_2O_2 + H^+$ requires 255.1128).

A solution of 1-chloro-3-iodobenzene (49 mg, 0.205 mmol) in anhydrous THF (0.5 mL) was treated with $PdCl_2(PPh_3)_2$ (7 mg, 0.01 mmol). After the resulting solution was stirred for 5 min at 25 °C, Et_3N (0.2 mL, 0.603 mmol) and CuI (10 mg, 0.053 mmol) were added. The suspension was stirred for 35 min, and **3b** (30 mg, 0.067 mmol) was added. After being stirred for 14 h at 25 °C, the reaction mixture was filtered through Celite and concentrated. PTLC (SiO_2, 50% EtOAc−hexanes) afforded 1-oxo-1-[5-(2-pyridyl)oxazol-2-yl]-7-(3-chlorophenyl)hept-6-yne (**4hh**; 24 mg, 0.066 mmol, 56%) as a yellow solid: mp 50−51 °C; ^{1}H NMR ($CDCl_3$, 500 MHz) δ 8.68−8.66 (m, 1H), 7.89−7.86 (m, 2H), 7.82 (td, 1H, $J = 7.7$, 1.8 Hz), 7.38 (m, 1H), 7.34−7.31 (m, 1H), 7.27−7.18 (m, 3H), 3.20 (t, 2H, $J = 7.4$ Hz), 2.49 (t 2H, $J = 7.0$ Hz), 2.00−1.95 (m, 2H), 1.77−1.71 (m, 2H); ^{13}C NMR ($CDCl_3$, 125 MHz) δ 187.9, 157.2, 153.3, 150.1, 146.2, 137.1, 133.9, 131.4, 129.6, 129.3, 127.8, 126.8, 125.5, 124.1, 120.3, 90.9, 79.8, 38.5, 27.8, 23.1, 19.1; IR (film) ν_{max} 3061, 2932, 2865, 2230, 1703, 1592, 1575, 1558, 1505, 1471, 1426, 1385, 1283, 1243, 1152, 1081, 1065, 1023, 990, 962, 930, 880, 784, 740, 683 cm^{-1}; ESI-TOF-MS *m*/*z* 365.1058 ($C_{21}H_{17}ClN_2O_4 + H^+$ requires 365.1051).

A solution of **4hh** (15 mg, 0.041 mmol) in anhydrous THF (1 mL) was treated with a catalytic amount of Raney nickel (washed before use with THF). The reaction mixture was purged with H_2 and stirred at 25 °C overnight. The suspension was filtered through Celite and concentrated. The crude product was dissolved in anhydrous CH_2Cl_2 (2 mL) and treated with Dess−Martin reagent (29 mg, 0.068 mmol). After being stirred for 3 h at 25 °C, the reaction mixture was quenched with saturated aqueous Na_2CO_3 and saturated aqueous $Na_2S_2O_3$. After being stirred for 15 min, the mixture was extracted with CH_2Cl_2. The organic layer was dried over Na_2SO_4, filtered, and concentrated. PTLC (SiO_2, 40% EtOAc−hexanes) afforded the title compound **5hh** (10 mg, 0.027 mmol, 67%) as a white solid: mp 91−92 °C; ^{1}H NMR ($CDCl_3$, 600 MHz) δ 8.68−8.66 (m, 1H), 7.89−7.86 (m, 2H), 7.82 (td, 1H, $J = 7.8$, 1.4 Hz), 7.34−7.31 (m, 1H), 7.21−7.14 (m, 3H), 7.04 (d, 1H, $J = 7.5$ Hz), 3.11 (t, 2H, $J = 7.4$ Hz), 2.59 (t, 2H, $J = 7.4$ Hz), 1.81−1.76 (m, 2H), 1.65−1.60 (m, 2H), 1.46−1.36 (m, 4H); ^{13}C NMR ($CDCl_3$, 125 MHz) δ 188.4, 157.3, 153.2, 150.1, 146.3, 144.7, 137.1, 133.9, 129.5, 128.5, 126.8, 126.6, 124.1, 120.4, 39.0, 35.5, 31.0, 28.9, 28.8, 23.8; IR (film) ν_{max} 2930, 2856, 1698, 1601, 1575, 1505, 1470, 1426, 1385, 1285, 1081, 1035, 990, 962, 935, 783, 741, 696 cm^{-1}; ESI-TOF-MS *m*/*z* 369.1363 ($C_{21}H_{21}ClN_2O_2 + H^+$ requires 369.1364).

1-Oxo-1-[5-(2-pyridyl)oxazol-2-yl]-3-(4-(benzyloxy)phenyl)-propane (11a). 4-Hydroxycinnamic acid (700 mg, 4.26 mmol) was dissolved in EtOAc (15 mL), and 10% Pd/C (51 mg, 0.479 mmol) was added. The reaction mixture was stirred under an atmosphere of H_2 overnight at room temperature before it was filtered through Celite and concentrated in vacuo. No further purification was needed to yield 3-(4-hydroxyphenyl)propanoic acid (700 mg, 99%). A solution of 3-(4-hydroxyphenyl)propanoic acid (700 mg, 4.21 mmol) in anhydrous DMF (16 mL) at 0 °C was treated with a solution of 60% NaH (450 mg, 18.75 mmol) in DMF dropwise. The reaction mixture was stirred for 10 min before benzyl bromide (0.675 mL, 5.68 mmol) was added. The reaction mixture was stirred overnight at room temperature, quenched with aqueous 1 N HCl, and extracted with EtOAc. The combined organic layers were washed with saturated aqueous NH_4Cl and saturated aqueous NaCl and dried over Na_2SO_4. Column chromatography (SiO_2, 4 × 9 cm, 20−40% EtOAc−hexanes gradient) afforded 3-(4-(benzyloxy)-phenyl)propanoic acid (780 mg, 72%) as a white solid: ^{1}H NMR ($CDCl_3$, 500 MHz) δ 7.44 (d, 2H, $J = 7.4$ Hz), 7.40 (t, 2H, $J = 7.4$ Hz), 7.35−7.32 (m, 1H), 7.14 (d, 2H, $J = 8.8$ Hz), 6.92 (d, 2H, $J = 8.4$ Hz), 5.06 (s, 2H), 2.92 (t, 2H, $J = 7.7$ Hz), 2.66 (t, 2H, $J = 7.7$ Hz); ^{13}C NMR ($CDCl_3$, 125 MHz) δ 179.0, 157.3, 137.0, 132.5, 129.2, 128.5, 127.9, 127.4, 114.9, 70.0, 35.8, 29.7.

A solution of **6**[72] (116 mg, 0.794 mmol) in anhydrous THF (4 mL) at −78 °C was treated dropwise with a solution of *n*-BuLi in hexanes (1.6 M, 0.64 mL, 0.953 mmol) under N_2, and the resulting solution was stirred at −78 °C for 35 min. A solution of $ZnCl_2$ in THF (0.5 M, 1.9 mL, 1.56 mmol) was added, and the mixture was allowed to warm to 0 °C. After the mixture was stirred at 0 °C for 45 min, CuI (160 mg, 0.840 mmol) was added. After the mixture was stirred at 0 °C for 15 min, a solution of 3-(4-hydroxyphenyl)-propanoyl chloride (1.2 equiv, prepared from 3-(4-(benzyloxy)-phenyl)propanoic acid and oxalyl chloride) in anhydrous THF (1.5 mL) was added dropwise, and the mixture was stirred for an additional 1 h. The reaction mixture was quenched with addition of saturated aqueous $NaHCO_3$ and extracted with EtOAc. The organic layer was filtered through Celite, dried over anhydrous Na_2SO_4, filtered, and evaporated to yield the crude product. Column chromatography (SiO_2, 2.5 × 5 cm, 10−30% EtOAc−hexanes gradient) followed by PTLC (SiO_2, 50% EtOAc−hexanes) afforded the title compound **11a** (33%) as a white solid: mp 99−100 °C; ^{1}H NMR ($CDCl_3$, 400 MHz) δ 8.67 (app d, J = 4.4 Hz, 1H), 7.88 (s, 1H), 7.87−7.85 (m, 1H), 7.81 (td, 1H, J = 7.8, 1.8 Hz), 7.44 (d, 2H, J = 7.0 Hz), 7.39 (t, 2H, J = 7.5 Hz), 7.32 (t, 2H, J = 6.8 Hz), 7.19 (d, 2H, J = 8.5 Hz), 6.91 (d, 2H, J = 8.5 Hz), 5.04 (s, 2H), 3.44 (t, 2H, J = 7.4 Hz), 3.06 (t, 2H, J = 7.4 Hz); ^{13}C NMR ($CDCl_3$, 100 MHz) δ 187.4, 157.2 (2C), 153.2, 150.1, 146.2, 137.1, 137.0, 132.7, 129.4, 128.5, 127.9, 127.4, 126.9, 124.2, 120.4, 114.9, 70.0, 40.9, 28.9; IR (film) ν_{max} 3097, 2919, 1693, 1602, 1582, 1514, 1470, 1427, 1382, 1253, 1177, 1042, 963, 938, 785, 741, 697 cm^{-1}; ESI-TOF-MS m/z 385.1549 ($C_{24}H_{20}N_2O_3 + H^+$ requires 385.1547).

FAAH Inhibition. ^{14}C-labeled oleamide was prepared from ^{14}C-labeled oleic acid as described.[12] The truncated rat FAAH (rFAAH) was expressed in *E. coli* and purified as described.[79] The purified recombinant rFAAH was used in the inhibition assays unless otherwise indicated. The full-length human FAAH (hFAAH) was expressed in COS-7 cells as described,[3] and the lysate of hFAAH-transfected COS-7 cells was used in the inhibition assays where explicitly indicated.

The inhibition assays were performed as described.[12] In brief, the enzyme reaction was initiated by mixing 1 nM rFAAH (800, 500, or 200 pM rFAAH for inhibitors with $K_i \leq 1-2$ nM) with 10 μM ^{14}C-labeled oleamide in 500 μL of reaction buffer (125 mM TrisCl, 1 mM EDTA, 0.2% glycerol, 0.02% Triton X-100, 0.4 mM Hepes, pH 9.0) at room temperature in the presence of three different concentrations of inhibitor. The enzyme reaction was terminated by transferring 20 μL of the reaction mixture to 500 μL of 0.1 N HCl at three different time points. The ^{14}C-labeled oleamide (substrate) and oleic acid (product) were extracted with EtOAc and analyzed by TLC as detailed.[12] The K_i of the inhibitor was calculated using a Dixon plot as described (standard deviations are provided in the Supporting Information tables).[47] Lineweaver−Burk analysis was performed as described, confirming competitive, reversible inhibition.[45]

Selectivity Screening. The selectivity screening was conducted as detailed.[70]

Acknowledgment. We gratefully acknowledge the financial support of the National Institutes of Health (Grant DA15648, D.L.B.; Grants DA017259 and DA015197, B.F.C.) and the Skaggs Institute for Chemical Biology and the postdoctoral fellowship support for F.A.R. (American Cancer Society).

Supporting Information Available: Full experimental details and characterization, FAAH assay measurement errors, and purities (HPLC analysis) of the FAAH inhibitors disclosed herein. This information is available free of charge via the Internet at http://pubs.acs.org.

References

(1) Bracey, M. H.; Hanson, M. A.; Masuda, K. R.; Stevens, R. C.; Cravatt, B. F. Structural Adaptations in a Membrane Enzyme That Terminates Endocannabinoid Signaling. *Science* **2002**, *298*, 1793−1796.

(2) Cravatt, B. F.; Giang, D. K.; Mayfield, S. P.; Boger, D. L.; Lerner, R. A.; Gilula, N. B. Molecular Characterization of an Enzyme That Degrades Neuromodulatory Fatty Acid Amides. *Nature* **1996**, *384*, 83−87.

(3) Giang, D. K.; Cravatt, B. F. Molecular Characterization of Human and Mouse Fatty Acid Amide Hydrolases. *Proc. Natl. Acad. Sci. U.S.A.* **1997**, *94*, 2238−2242.

(4) Patricelli, M. P.; Cravatt, B. F. Proteins Regulating the Biosynthesis and Inactivation of Neuromodulatory Fatty Acid Amides. *Vitam. Horm.* **2001**, *62*, 95−131.

(5) Egertova, M.; Cravatt, B. F.; Elphick, M. R. Comparative Analysis of Fatty Acid Amide Hydrolase and CB1 Cannabinoid Receptor Expression in the Mouse Brain: Evidence of a Widespread Role for Fatty Acid Amide Hydrolase in Regulation of Endocannabinoid Signaling. *Neuroscience* **2003**, *119*, 481−496.

(6) Patricelli, M. P.; Cravatt, B. F. Fatty Acid Amide Hydrolase Competitively Degrades Bioactive Amides and Esters through a Nonconventional Catalytic Mechanism. *Biochemistry* **1999**, *38*, 14125−14130.

(7) Patricelli, M. P.; Cravatt, B. F. Clarifying the Catalytic Roles of Conserved Residues in the Amidase Signature Family. *J. Biol. Chem.* **2000**, *275*, 19177−19184.

(8) Patricelli, M. P.; Lovato, M. A.; Cravatt, B. F. Chemical and Mutagenic Investigations of Fatty Acid Amide Hydrolase: Evidence for a Family of Serine Hydrolases with Distinct Catalytic Properties. *Biochemistry* **1999**, *38*, 9804−9812.

(9) Devane, W. A.; Hanus, L.; Breuer, A.; Pertwee, R. G.; Stevenson, L. A.; Griffin, G.; Gibson, D.; Mandelbaum, A.; Etinger, A.; Mechoulam, R. Isolation and Structure of a Brain Constituent That Binds to the Cannabinoid Receptor. *Science* **1992**, *258*, 1946−1949.

(10) Boger, D. L.; Henriksen, S. J.; Cravatt, B. F. Oleamide: An Endogenous Sleep-Inducing Lipid and Prototypical Member of a New Class of Lipid Signalling Molecules. *Curr. Pharm. Des.* **1998**, *4*, 303−314.

(11) Cravatt, B. F.; Lerner, R. A.; Boger, D. L. Structure Determination of an Endogenous Sleep-Inducing Lipid, *cis*-9-Octadecenamide (Oleamide): A Synthetic Approach to the Chemical Analysis of Trace Quantitites of a Natural Product. *J. Am. Chem. Soc.* **1996**, *118*, 580−590.

(12) Cravatt, B. F.; Prospero-Garcia, O.; Suizdak, G.; Gilula, N. B.; Henriksen, S. J.; Boger, D. L.; Lerner, R. A. Chemical Characterization of a Family of Brain Lipids That Induce Sleep. *Science* **1995**, *268*, 1506−1509.

(13) Boger, D. L.; Fecik, R. A.; Patterson, J. E.; Miyauchi, H.; Patricelli, M. P.; Cravatt, B. F. Fatty Acid Amide Hydrolase Substrate Specificity. *Bioorg. Med. Chem. Lett.* **2000**, *10*, 2613−2616.

(14) Lang, W.; Qin, C.; Lin, S.; Khanolkar, A. D.; Goutopoulos, A.; Fan, P.; Abouzid, K.; Meng, Z.; Biegel, D.; Makriyannis, A. Substrate Specificity and Stereoselectivity of Rat Brain Microsomal Anandamide Amidohydrolase. *J. Med. Chem.* **1999**, *42*, 896−902.

(15) Schmid, H. H. O.; Schmid, P. C.; Natarajan, V. *N*-Acylated Glycerophospholipids and Their Derivatives. *Prog. Lipid Res.* **1990**, *29*, 1−43.

(16) Lambert, D. M.; Fowler, C. J. The Endocannabinoid System: Drug Targets, Lead Compounds, and Potential Therapeutic Applications. *J. Med. Chem.* **2005**, *48*, 5059−5087.

(17) Calignano, A.; La Rana, G.; Giuffrida, A.; Piomelli, D. Control of Pain Initiation by Endogenous Cannabinoids. *Nature* **1998**, *394*, 277−281.

(18) Cravatt, B. F.; Lichtman, A. H. The Endogenous Cannabinoid System and Its Role in Nociceptive Behavior. *J. Neurobiol.* **2004**, *61*, 149−160.

(19) Walker, J. M.; Huang, S. M.; Stragman, N. M.; Tsou, K.; Sanudo-Pena, M. C. Pain Modulation by Release of the Endogenous Cannabinoid Anamdamide. *Proc. Natl. Acad. Sci. U.S.A.* **1999**, *96*, 12198−12203.

(20) Gomez, R.; Navarro, M.; Ferrer, B.; Trigo, J. M.; Bilbao, A.; Del Arco, I.; Cippitelli, A.; Nava, F.; Piomelli, D.; Rodríguez de Fonseca, F. A Peripheral Mechanism for CB1 Cannabinoid Receptor Dependent Modulation of Feeding. *J. Neurosci.* **2002**, *22*, 9612−9617.

(21) Williams, C. M.; Kirkham, T. C. Observational Analysis of Feeding Induced by Δ-THC and Anandamide. *Physiol. Behav.* **2002**, *76*, 241−250.

(22) Kathuria, S.; Gaetani, S.; Fegley, D.; Valino, F.; Duranti, A.; Tontini, A.; Mor, M.; Tarzia, G.; La Rana, G.; Calignano, A.; Giustino, A.; Tattoli, M.; Palmery, M.; Cuomo, V.; Piomelli, D. Modulation of Anxiety Through Blockade of Anandamide Hydrolysis. *Nat. Med.* **2003**, *9*, 76−81.

(23) Melck, D.; Rueda, D.; Galve-Roberh, I.; De Petrocellis, L.; Guzmán, M.; Di Marzo, V. Involvement of the cAMP/Protein Kinase A Pathway and of Mitogen-Activated Protein Kinase in the Anti-Proliferative Effects of Anandamide in Human Breast Cancer Cells. *FEBS Lett.* **1999**, *463*, 235−240.

(24) Yamaji, K.; Sarker, K. P.; Kawahara, K.; Iino, S.; Yamakuchi, M.; Abeyama, K.; Hashiguchi, T.; Maruyama, I. Anandamide Induces Apoptosis in Human Endothelial Cells: Its Regulation System and Clinical Implications. *Thromb. Haemostasis* **2003**, *89*, 875−884.
(25) Massa, F.; Marsicano, G.; Hermann, H.; Cannich, A.; Monory, K.; Cravatt, B. F.; Ferri, G. L.; Sibaev, A.; Storr, M.; Lutz, B. The Endogenous Cannabinoid System Protects against Colonic Inflammation. *J. Clin. Invest.* **2004**, *113*, 1202−1209.
(26) Mallet, P. E.; Beninger, R. J. The Cannabinoid CB1 Receptor Antagonist SR141716A Attenuates the Memory Impairment Produced by Δ9-Tetrahydrocannabinol or Anandamide. *Psychopharmacology* **1998**, *140*, 11−19.
(27) Panikashvili, D.; Simeonidou, C.; Ben Shabat, S.; Hanus, L.; Breuer, A.; Mechoulam, R.; Shohami, E. An Endogenous Cannabinoid (2-AG) is Neuroprotective after Brain Injury. *Nature* **2001**, *413*, 527−531.
(28) Axelrod, J.; Felder, C. C. Cannabinoid Receptors and Their Endogenous Agonist, Anandamide. *Neurochem. Res.* **1998**, *23*, 575−581.
(29) Di Marzo, V.; Bisogno, T.; De Petrocellis, L.; Melck, D.; Martin, B. R. Cannabimimetic Fatty Acid Derivatives: The Anandamide Family and Other "Endocannabinoids." *Curr. Med. Chem.* **1999**, *6*, 721−744.
(30) Martin, B. R.; Mechoulam, R.; Razdan, R. K. Discovery and Characterization of Endogenous Cannabinoids. *Life Sci.* **1999**, *65*, 573−595.
(31) Cheer, J. F.; Cadogan, A. K.; Marsden, C. A.; Fone, K. C. F.; Kendall, D. A. Modification of 5-HT2 Receptor Mediated Behaviour in the Rat by Oleamide and the Role of Cannabinoid Receptors. *Neuropharmacology* **1999**, *38*, 533−541.
(32) Thomas, E. A.; Cravatt, B. F.; Sutcliffe, J. G. The Endogenous Lipid Oleamide Activates Serotonin 5-HT7 Neurons in Mouse Thalamus and Hypothalamus. *J. Neurochem.* **1999**, *72*, 2370−2378.
(33) Boger, D. L.; Patterson, J. E.; Jin, Q. Structural Requirements for 5-HT2A and 5-HT1A Receptor Potentiation by the Biologically Active Lipid Oleamide. *Proc. Natl. Acad. Sci. U.S.A.* **1998**, *95*, 4102−4107.
(34) Lees, G.; Dougalis, A. Differential Effects of the Sleep-Inducing Lipid Oleamide and Cannabinoids on the Induction of Long-Term Potentiation in the CA1 Neurons of the Rat Hippocampus in Vitro. *Brain Res.* **2004**, *997*, 1−14.
(35) Yost, C. S.; Hampson, A. J.; Leonoudakis, D.; Koblin, D. D.; Bornheim, L. M.; Gray, A. T. Oleamide Potentiates Benzodiazepine-Sensitive γ-Aminobutyric Acid Receptor Activity but Does Not Alter Minimum Alveolar Anesthetic Concentration. *Anesth. Analg.* **1998**, *86*, 1294−1299.
(36) Huitrón-Reséndiz, S.; Gombart, L.; Cravatt, B. F.; Henriksen, S. J. Effect of Oleamide on Sleep and Its Relationship to Blood Pressure, Body Temperature, and Locomotor Activity in Rats. *Exp. Neurol.* **2001**, *172*, 235−243.
(37) Boger, D. L.; Patterson, J. E.; Guan, X.; Cravatt, B. F.; Lerner, R. A.; Gilula, N. B. Chemical Requirements for Inhibition of Gap Junction Communication by the Biologically Active Lipid Oleamide. *Proc. Natl. Acad. Sci. U.S.A.* **1998**, *95*, 4810−4815.
(38) Guan, X.; Cravatt, B. F.; Ehring, G. R.; Hall, J. E.; Boger, D. L.; Lerner, R. A.; Gilula, N. B. The Sleep-Inducing Lipid Oleamide Deconvolutes Gap Junction Communication and Calcium Wave Transmission in Glial Cells. *J. Cell Biol.* **1997**, *139*, 1785−1792.
(39) Mechoulam, R.; Fride, E.; Hanus, L.; Sheskin, T.; Bisogno, T.; Di Marzo, V.; Bayewitch, M.; Vogel, Z. Anandamide May Mediate Sleep Induction. *Nature* **1997**, *389*, 25−26.
(40) Clement, A. B.; Hawkins, E. G.; Lichtman, A. H.; Cravatt, B. F. Increased Seizure Susceptibility and Proconvulsant Activity of Anandamide in Mice Lacking Fatty Acid Amide Hydrolase. *J. Neurosci.* **2003**, *23*, 3916−3923.
(41) Cravatt, B. F.; Demarest, K.; Patricelli, M. P.; Bracey, M. H.; Giang, D. K.; Martin, B. R.; Lichtman, A. H. Supersensitivity to Anandamide and Enhanced Endogenous Cannabinoid Signaling in Mice Lacking Fatty Acid Amide Hydrolase. *Proc. Natl. Acad. Sci. U.S.A.* **2001**, *98*, 9371−9376.
(42) Cravatt, B. F.; Saghatelian, A.; Hawkins, E. G.; Clement, A. B.; Bracey, M. H.; Lichtman, A. H. Functional Disassociation of the Central and Peripheral Fatty Acid Amide Signaling Systems. *Proc. Natl. Acad. Sci. U.S.A.* **2004**, *101*, 10821−10826.
(43) Lichtman, A. H.; Shelton, C. C.; Advani, T.; Cravatt, B. F. Mice Lacking Fatty Acid Amide Hydrolase Exhibit a Cannabinoid Receptor-Mediated Phenotypic Hypoalgesia. *Pain* **2004**, *109*, 319−327.
(44) Cravatt, B. F.; Lichtman, A. H. Fatty Acid Amide Hydrolase: An Emerging Therapeutic Target in the Endocannabinoid System. *Curr. Opin. Chem. Biol.* **2003**, *7*, 469−475.
(45) Boger, D. L.; Miyauchi, H.; Du, W.; Hardouin, C.; Fecik, R. A.; Cheng, H.; Hwang, I.; Hedrick, M. P.; Leung, D.; Acevedo, O.; Guimaráes, C. R. W.; Jorgensen, W. L.; Cravatt, B. F. Discovery of a Potent, Selective, and Efficacious Class of Reversible α-Ketoheterocycle Inhibitors of Fatty Acid Amide Hydrolase as Analgesics. *J. Med. Chem.* **2005**, *48*, 1849−1856.
(46) Boger, D. L.; Sato, H.; Lerner, A. E.; Austin, B. J.; Patterson, J. E.; Patricelli, M. P.; Cravatt, B. F. Trifluoromethyl Ketone Inhibitors of Fatty Acid Amide Hydrolase: A Probe of Structural and Conformational Features Contributing to Inhibition. *Bioorg. Med. Chem. Lett.* **1999**, *9*, 265−270.
(47) Boger, D. L.; Sato, H.; Lerner, A. E.; Hedrick, M. P.; Fecik, R. A.; Miyauchi, H.; Wilkie, G. D.; Austin, B. J.; Patricelli, M. P.; Cravatt, B. F. Exceptionally Potent Inhibitors of Fatty Acid Amide Hydrolase: The Enzyme Responsible for Degradation of Endogenous Oleamide and Anandamide. *Proc. Natl. Acad. Sci. U.S.A.* **2000**, *97*, 5044−5049.
(48) De Petrocellis, L.; Melck, D.; Ueda, N.; Maurelli, S.; Kurahashi, Y.; Yamamoto, S.; Marino, G.; Di Marzo, V. Novel Inhibitors of Brain, Neuronal, and Basophilic Anandamide Amidohydrolase. *Biochem. Biophys. Res. Commun.* **1997**, *231*, 82−88.
(49) Deutsch, D. G.; Omeir, R.; Arreaza, G.; Salehani, D.; Prestwich, G. D.; Huang, Z.; Howlett, A. Methyl Arachidonyl Fluorophosphonate: A Potent Irreversible Inhibitor of Anandamide Amidase. *Biochem. Pharmacol.* **1997**, *53*, 255−260.
(50) Deutsch, D. G.; Lin, S.; Hill, W. A. G.; Morse, K. L.; Salehani, D.; Arreaza, G.; Omeir, R. L.; Makriyannis, A. Fatty Acid Sulfonyl Fluorides Inhibit Anandamide Metabolism and Bind to the Cannabinoid Receptor. *Biochem. Biophys. Res. Commun.* **1997**, *231*, 217−221.
(51) Du, W.; Hardouin, C.; Cheng, H.; Hwang, I.; Boger, D. L. Heterocyclic Sulfoxide and Sulfone Inhibitors of Fatty Acid Amide Hydrolase. *Bioorg. Med. Chem. Lett.* **2005**, *15*, 103−106.
(52) Edgemond, W. S.; Greenberg, M. J.; McGinley, P. J.; Muthians, S.; Campbell, W. B.; Hillard, C. J. Synthesis and Characterization of Diazomethylarachidonyl Ketone: An Irreversible Inhibitor of *N*-Arachidonylethanolamine Amidohydrolase. *J. Pharmacol. Exp. Ther.* **1998**, *286*, 184−190.
(53) Fernando, S. R.; Pertwee, R. G. Evidence That Methyl Arachidonyl Fluorophosphonate Is an Irreversible Cannabinoid Receptor Antagonist. *Br. J. Pharmacol.* **1997**, *121*, 1716−1720.
(54) Koutek, B.; Prestwich, G. D.; Howlett, A. C.; Chin, S. A.; Salehani, D.; Akhavan, N.; Deutsch, D. G. Inhibitors of Arachidonoyl Ethanolamide Hydrolysis. *J. Biol. Chem.* **1994**, *269*.
(55) Patricelli, M. P.; Patterson, J. P.; Boger, D. L.; Cravatt, B. F. An Endogenous Sleep-Inducing Compound Is a Novel Competitive Inhibitor of Fatty Acid Amide Hydrolase. *Bioorg. Med. Chem. Lett.* **1998**, *8*, 613−618.
(56) Patterson, J. E.; Ollmann, I. R.; Cravatt, B. F.; Boger, D. L.; Wong, C.-H.; Lerner, R. A. Inhibition of Oleamide Hydrolase Catalyzed Hydrolysis of the Endogenous Sleep-Inducing Lipid cis-9-Octadecenamide. *J. Am. Chem. Soc.* **1996**, *1996*, 5938−5945.
(57) Tarzia, G.; Duranti, A.; Gatti, G.; Piersanti, G.; Tontini, A.; Rivara, S.; Lodola, A.; Plazzi, P. V.; Mor, M.; Kathuria, S.; Piomelli, D. Synthesis and Structure−Activity Relationships of FAAH Inhibitors: Cyclohexylcarbamic Acid Biphenyl Esters with Chemical Modulation at the Proximal Phenyl Ring. *ChemMedChem* **2006**, *1*, 130−139.
(58) Tarzia, G.; Duranti, A.; Tontini, A.; Piersanti, G.; Mor, M.; Rivara, S.; Plazzi, P. V.; Park, C.; Kathuria, S.; Piomelli, D. Design, Synthesis, and Structure-Activity Relationships of Alkylcarbamic Acid Aryl Esters, a New Class of Fatty Acid Amide Hydrolase Inhibitors. *J. Med. Chem.* **2003**, *46*, 2352−2360.
(59) Mor, M.; Rivara, S.; Lodola, A.; Plazzi, P. V.; Tarzia, G.; Duranti, A.; Tontini, A.; Piersanti, G.; Kathuria, S.; Piomelli, D. Cyclohexylcarbamic Acid 3′- or 4′-Substituted Biphenyl-3-yl Esters as Fatty Acid Amide Hydrolase Inhibitors: Synthesis, Quantitative Structure−Activity Relationships, and Molecular Modeling Studies. *J. Med. Chem.* **2004**, *47*, 4998−5008.
(60) Muccioli, G. G.; Fazio, N.; Scriba, G. K. E.; Poppitz, W.; Cannata, F.; Poupaert, J. H.; Wouters, J.; Lambert, D. M. Substituted 2-Thioxoimidazolidin-4-ones and Imidazolidine-2,4-diones as Fatty Acid Amide Hydrolase Inhibitors Templates. *J. Med. Chem.* **2006**, *49*, 417−425.
(61) Leung, D.; Du, W.; Hardouin, C.; Cheng, H.; Hwang, I.; Cravatt, B. F.; Boger, D. L. Discovery of an Exceptionally Potent and Selective Class of Fatty Acid Amide Hydrolase Inhibitors Enlisting Proteome-Wide Selectivity Screening: Concurrent Optimization of Enzyme Inhibitor Potency and Selectivity. *Bioorg. Med. Chem. Lett.* **2005**, *15*, 1423−1428.

(62) Hohmann, A. G.; Suplita, R. L.; Bolton, N. M.; Neeley, M. H.; Fegley, D.; Mangieri, R.; Krey, J.; Walker, J. M.; Holmes, P. V.; Crystal, J. D.; Duranti, A.; Tontini, A.; Mor, M.; Tarzia, G.; Piomelli, D. An Endocannabinoid Mechanism for Stress-Induced Analgesia. *Nature* **2005**, *435*, 1108−1112.

(63) Alexander, J. P.; Cravatt, B. F. Mechanism of Carbamate Inactivation of FAAH: Implications for the Design of Covalent Inhibitors and in Vivo Functional Probes for Enzymes. *Chem. Biol.* **2005**, *12*, 1179−1187.

(64) Lichtman, A. H.; Leung, D.; Shelton, C. C.; Saghatelian, A.; Hardouin, C.; Boger, D. L.; Cravatt, B. F. Reversible Inhibitors of Fatty Acid Amide Hydrolase That Promote Analgesia: Evidence for an Unprecedented Combination of Potency and Selectivity. *J. Pharmacol. Exp. Ther.* **2004**, *311*, 441−448. See also: Zhang, D.; Saraf, A.; Kolasa, T.; Bhatia, P.; Zheng, G. Z.; Patel, M.; Lannoye, G. S.; Richardson, P.; Stewart, A.; Rogers, J. C.; Brioni, J. D.; Surowy, C. S. Fatty Acid Amide Hydrolase Inhibitors Display Broad Selectivity and Inhibit Multiple Carboxylesterases as Off-Targets. *Neuropharmacology*, in press.

(65) Alexander, J. P.; Cravatt, B. F. The Putative Endocannabinoid Transport Blocker LY2183240 Is a Potent Inhibitor of FAAH and Several Other Brain Serine Hydrolases. *J. Am. Chem. Soc.* **2006**, *128*, 9699−9704.

(66) Boger, D. L.; Miyauchi, H.; Hedrick, M. P. α-Keto Heterocycle Inhibitors of Fatty Acid Amide Hydrolase: Carbonyl Group Modification and α-Substitution. *Bioorg. Med. Chem. Lett.* **2001**, *11*, 1517−1520.

(67) Chang, L.; Luo, L.; Palmer, J. A.; Sutton, S.; Wilson, S. J.; Barbier, A. J.; Breitenbucher, J. G.; Chaplan, S. R.; Webb, M. Inhibition of Fatty Acid Amide Hydrolase Produces Analgesia by Multiple Mechanisms. *Br. J. Pharmacol.* **2006**, *148*, 102−113.

(68) Romero, F. A.; Hwang, I.; Boger, D. L. Delineation of a Fundamental α-Ketoheterocycle Substituent Effect for Use in the Design of Enzyme Inhibitors. *J. Am. Chem. Soc.* **2006**, *68*, 14004−14005.

(69) Romero, F. A.; Du, W.; Hwang, I.; Rayl, T. J.; Leung, D.; Hoover, H. S.; Cravatt, B. F.; Boger, D. L. Potent and Selective α-Ketoheterocycle-Based Inhibitors of the Anandamide and Oleamide Catabolizing Enzyme, Fatty Acid Amide Hydrolase. *J. Med. Chem.* **2007**, *50*, 1058−1068.

(70) Leung, D.; Hardouin, C.; Boger, D. L.; Cravatt, B. F. Discovering Potent and Selective Reversible Inhibitors of Enzymes in Complex Proteomes. *Nat. Biotechnol.* **2003**, *21*, 687−691.

(71) Sonogashira, K.; Tohda, Y.; Hagihara, N. A Convenient Synthesis of Acetylenes: Catalytic Substitutions of Acetylenic Hydrogen with Bromoalkenes, Iodoarenes, and Bromopyridines. *Tetrahedron Lett.* **1975**, *16*, 4467−4470.

(72) Saikachi, H.; Kitagawa, T.; Sasaki, H.; Van Leusen, A. M. Synthesis of Furan Derivatives. LXXXV. Condensation of Heteroaromatic Aldehydes with Tosylmethyl Isocyanide. *Chem. Pharm. Bull.* **1969**, *27*, 793−796.

(73) Harn, N. K.; Gramer, C. J.; Anderson, B. A. Acylation of Oxazoles by the Copper-Mediated Reaction of Oxazol-2-ylzinc Chloride Derivatives. *Tetrahedron Lett.* **1995**, *36*, 9453−9456.

(74) Dondoni, A.; Fantin, G.; Fogagnolo, M.; Medici, A.; Pedrini, P. Synthesis of (Trimethylsily1)thiazoles and Reactions with Carbonyl Compounds. Selectivity Aspects and Synthetic Utility. *J. Org. Chem.* **1988**, *53*, 1748−1761.

(75) Dondoni, A.; Mastellari, A. R.; Medici, A.; Negrini, E.; Pedrini, P. Synthesis of Stannylthiazoles and Mixed Stannylsilylthiazoles and Their Use for a Convenient Preparation of Mono- and Bis-Halothiazoles. *Synthesis* **1986**, 757−760.

(76) Pocar, D.; Stradi, R.; Trimarco, P. Enamines from Cyclopropylketones. *Tetrahedron* **1975**, *31*, 2427−2429.

(77) Yovell, J.; Hirsch, D.; Sarel, S. Acid-Catalyzed Addition of Secondary Amines to Cyclopropyl Ketones. Mass Spectra of Some Cyclic Aminobutyrophenones. *J. Org. Chem.* **1977**, *42*, 850−855.

(78) Davis, F. A.; Vishwakarma, L. C.; Billmers, J. M.; Finn, J. Synthesis of α-Hydroxy Carbonyl Compounds (Acyloins): Direct Oxidation of Enolates Using 2-Sulfonyloxaziridines. *J. Org. Chem.* **1984**, *49*, 3241−3243.

(79) Patricelli, M. P.; Lashuel, H. A.; Giang, D. K.; Kelly, J. W.; Cravatt, B. F. Comparative Characterization of a Wild Type and Transmembrane Domain-Deleted Fatty Acid Amide Hydrolase: Identification of the Transmembrane Domain as a Site for Oligomerization. *Biochemistry* **1998**, *37*, 15177−15187.

(80) For **2b**, MW = 334, four H-bond acceptors, and *c* log *P* = 4.12. For **5hh**, MW = 369, four H-bond acceptors, and *c* log *P* = 4.67. For **11j**, MW = 354, four H-bond acceptors, *c* log *P* = 4.12, and five rotatable bonds.

JM061414R